JOURNAL OF SPACECRAFT AND ROCKETS
Vol. 33, No. 6, November–December 1996

Five-Electron-Volt Atomic Oxygen Pulsed-Beam Characterization by Quadrupolar Mass Spectrometry

Bertrand Cazaubon,* Alain Paillous,† and Jean Siffre‡
Centre d'Etudes et de Recherches de Toulouse–ONERA, Toulouse 31055, France
and
Roger Thomas§
Laboratoire de Physique et Chimie de l'Environnement, Orléans 45071, France

The pulsed-beam source used to study the interaction of materials with 5-eV oxygen atoms of the low-Earth-orbit environment has been characterized by quadrupolar mass spectrometry. This technique permits a complete analysis of the pulsed beam, evidencing vacuum ultraviolet photons, ionic species O^+ and O_2^+, and neutral species O and O_2. Time-of-flight measurements allowed velocity distributions to be obtained and fluences to be calculated. In optimized working conditions delivering oxygen atoms at 8 km/s, the pulsed beam is composed of 90% oxygen atoms, with a fluence of 2.9 $\times 10^{15}$ atoms/cm^2 per shot at 40 cm from the source, 10% molecular oxygen at the average velocity 8 km/s, and a few parts per million of O^+ and O_2^+ at the same average velocity of about 11 km/s.

Nomenclature

d	= entrance orifice diameter of the ionization chamber, 2.5×10^{-3} m
d_e	= distance from ionization chamber to mass filter entrance, 2.5×10^{-2} m
d_q	= distance from quadrupolar mass filter to secondary-electrons multiplier, 2.44×10^{-1} m
d_0	= distance from nozzle to ionization chamber, 1 m
dt	= time between two consecutive points of the time scale, s
e	= elementary charge, 1.6×10^{-19} C
G	= gain of secondary-electrons multiplier
I	= ionization electronic current, 4×10^{-4} A
l	= average distance covered by electrons in the ionization chamber, 1 cm
m	= ionic mass, kg
$N_c(t)$	= quantity of cations produced by electron impact in the ionization chamber
$N_s(t)$	= particle flux at the spectrometer entrance, particles/cm^2
$N_v(t)$	= density of particles to be ionized is equal to $N_s(t)/v\ dt$, particles/m^3
$N_0(t)$	= quantity of charges at each point of the time distribution
n_e	= number of ionizing electrons, equal to $I\ dt/e$
p	= pressure in ionization chamber, 10^{-6} mbar
q	= ionic charge, C
R	= load resistance, Ω
s	= number of ions produced per electron, 3 ions $\cdot$ cm^{-1} $\cdot$ mbar^{-1} for 70-eV electron ionization energy
T	= transmission of the ion source in the mass spectrometer
$t_{oscillo}$	= time of flight measured between the VUV peak and specie peak, s
$V(t)$	= tension peak in each point of the time scale, V
$V_{Field\ Axis}$	= potential of the field-axis electrode, V
v	= velocity, m/s
v_0	= velocity of the considered species in the simulator, m/s
σ	= ionization cross section, m^2

Received Oct. 27, 1995; revision received April 15, 1996; accepted for publication May 5, 1996.

*Ph.D. Candidate, École Nationale Supérieure de l'Aéronautique et de l'Espace.
†Senior Research Engineer, Département d'Etudes et de Recherches en Technologie Spatiale, 2, av. Edouard Belin BP 4025. Member AIAA.
‡Member, Technical Staff.
§Engineer, 3, av. de la Recherche Scientifique.

Introduction

AT altitudes ranging from 200 to 700 km, especially during maximum solar activity periods, oxygen atoms in their ground state are the most abundant species of the space environment. In low Earth orbit (LEO), oxygen atoms interact with spacecraft leading-edge surfaces at the satellite velocity of about 8 km/s[1], which corresponds to a 5.3-eV kinetic energy of the oxygen atoms. In such conditions, spacecraft surfaces can be severely oxidized; material erosion and mass loss can be induced in some cases. To evaluate spacecraft material degradation, to understand damage mechanisms, and to develop new protective materials more resistant to the LEO environment, atomic-oxygen simulation facilities are required. Various high-velocity atomic-oxygen sources have been proposed.[1–6] The laser-assisted source developed by Caledonia et al.,[7] delivers a beam mainly composed of oxygen atoms with velocities that can be adjusted between 5 and 13 km/s, and fluxes varying from 10^{14} to 10^{16} atoms $\cdot$ cm^{-2} $\cdot$ s^{-1}, depending on the sample/source distance and the repetition rate. This source has been implemented in the atomic oxygen facility Chambre adaptée à l'Action de l'Oxygène Atomique sur les Revêtements (CASOAR) employed at Centre d'Etudes et de Recherches de Toulouse–ONERA.

To judge whether the laboratory simulation is suited to material testing, a complete knowledge of the beam is essential. A study performed by laser-induced fluorescence (LIF) has given us data concerning the time-of-flight (TOF) distribution and the fluence of oxygen atoms in ground state present in the beam.[8] The LIF method is characterized by a high selectivity and sensitivity, but observation of all species in the beam would require that a wide range of excitation wavelengths be scanned; moreover, the technique is complicated, difficult, and time-consuming. For more flexibility and simplicity, we have undertaken to characterize the atomic-oxygen pulsed beam by quadrupolar mass spectrometry, a device widely used to characterize the LEO environment[9–13] and products incoming from the interaction of atomic oxygen and materials exposed on the long-duration exposure facility[14] and Evaluation of Oxygen Interactions with Materials[15] experiments. We give experimental results obtained with this technique and describe the composition of the 5-eV beam delivered by the atomic-oxygen source of CASOAR.

Experiment

Atomic-Oxygen Source

The atomic-oxygen source used in CASOAR involves a pulsed-laser-induced breakdown of molecular oxygen. The simulation facility is described in Fig. 1. It consists of a cylindrical chamber, 60 cm in diameter and 60 cm high; samples up to 25 cm in diameter can be accommodated. High vacuum, in the 10^{-4} Pa range, is ensured by a 5000 l/s cryopump. The molecular oxygen, at a pressure of 2×10^6 Pa, is introduced into a conical nozzle of 20 deg total angle, through a rapid pulsed microvalve with 1-mm-diam orifice; the molecular-oxygen mass flow is 12 cm^3/min, for a 250-μs opening time of the microvalve and a pulse repetition rate of 1–3 Hz. A pulsed CO_2 laser is fired with a short time delay after the beginning of the valve opening. Atomic-oxygen velocities in the range of 5–13 km/s can be selected accurately by adjusting this time delay. The laser is a Coherent LT-612 pulsed CO_2 TEA laser at 10.6 μm, which delivers 10 J per pulse of 2-μs length. The laser beam is focused to a 6×4 mm spot in the throat of the nozzle, thanks to two gold-coated mirrors and a coated zinc selenide lens with an 85-cm focal length. The absorptive and reflective losses in the focusing optical system give a power density about 10^8 W/cm^2 per pulse in the nozzle. Two photomultipliers, located on the top flange of the source chamber, and separated by 7.6 cm, monitor the time of arrival of the peak of the 777.3-nm atomic-oxygen emission line. This optical measurement of TOF determines the velocity of the atomic oxygen in the $3p^5$P excited state present in the beam. More details on the technique can be found elsewhere.[7]

Quadrupole Mass Spectrometer

A Balzers QMA420 quadrupole mass spectrometer, located 100 cm from the nozzle and whose optical axis with the CO_2 laser beam forms an angle of 8 deg, was employed. High vacuum pumping of the mass spectrometer head is ensured by 400-l/s turbomolecular pumping to prevent background gas signals from confusing the measurements. A 2.5-mm-diam diaphragm is located 5 cm before the mass spectrometer entrance, to prevent pressure from rising above 10^{-2} Pa. The mass 2 spectrometer shown in Fig. 2 includes an ionization chamber where neutral species are ionized by crossed-beam electron impact. After formation, ions are transferred to the entrance of the quadrupole mass filter by means of ion optics. The ion optics are composed of an extraction electrode, two focusing lenses, and an accelerating electrode, so as to inject ions into the mass filter in the best filtering conditions, that is, in the center of the quadrupole and in parallel to the propagation axis. The quadrupole is composed of four cylindrical metal rods 20 cm long by 8 mm in diameter, where a sinusoidal voltage at 2.25 MHz is applied, enabling the scanning of a mass range of 1–512 amu. After transmission through the quadrupole, the ions are electrically detected, either by a Faraday cup, or by a secondary-electrons multiplier (SEM) following a 90-deg deflecting cylindrical condenser. Electrical signals from the detectors are measured as the terminal voltage on a load resistance on a 400-MHz digital oscilloscope. This load resistance must be high enough to visualize signals of a few millivolts, but, to avoid modification of the TOF distributions, the smallest possible to minimize the time constant of the measuring line. The mass spectrometer is controlled by software on a IBM/PS2 computer. The analog signals related to TOF and visualized on the digital oscilloscope are digitized and stored in files.

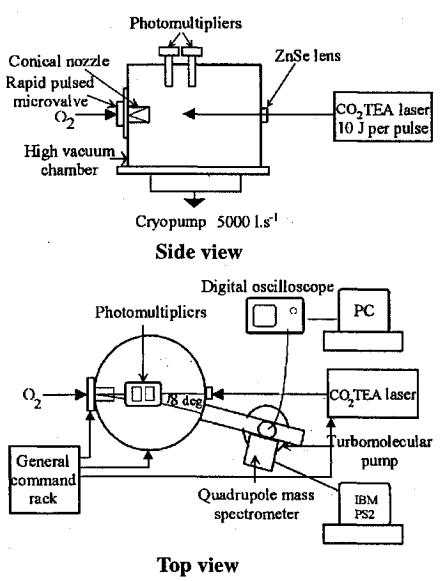

Fig. 1 CASOAR simulation chamber.

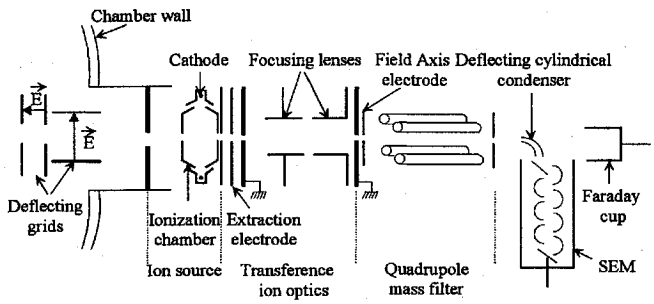

Fig. 2 Quadrupole mass spectrometer.

Characterization Methods of the Fast Atomic-Oxygen Beam

Velocity Measurement

Signals obtained on the oscilloscope give the TOF distribution of the filtered species between its formation in the nozzle and its detection by the SEM. When the CO_2 laser is fired, a signal spike is observed on the mass spectrometer detectors. This peak is present on the oscilloscope whatever mass the spectrometer is on, with or without emission of the ionizing electrons; it remains when a 300-V potential difference is applied on deflecting plates placed before the spectrometer entrance (see Fig. 2). These features strongly suggest that this signal is attributable to photon emission occurring during the plasma formation in the nozzle. To evaluate the wavelengths range of these photons, different windows have been placed in front of the spectrometer entrance. With a silica window allowing photons with wavelengths in the range from 250 to 3000 nm to pass through, the peak disappears entirely; with a magnesium fluoride window transmitting photons between 120 and 7000 nm, a part of the peak is still visualized. This indicates that these photons belong to the far uv, with wavelengths below 250 nm. A study realized at European Space Research and Technology Centre[16] with a similar atomic-oxygen source has shown that the spectral range of the photons emitted during the initial formation of the high-temperature plasma (20,000 K) extends from 60 to 300 nm with a maximum of intensity between 60 and 140 nm. Such photons have sufficient energy to make an electron photoemission on the conversion dynode of the SEM, after reflexion on metallic parts of the ion optics in the spectrometer. Although these vacuum ultraviolet (VUV) photons are disturbing the effects of atomic oxygen on materials are being studied, they can serve as time-zero markers of the formation of the plasma in the nozzle. The VUV signal also is used to evaluate the parasitic capacitor of the measuring line, by making the ratio of the voltages at 90 and 10% of the maximum value. With a 21.5-kΩ load resistance R, the measured parasitic capacitor is about 100 pF. Therefore, the time constant RC of the measuring line is about 2 μs, which is small enough to avoid modification of the TOF distributions of the different species visualized on the oscilloscope.

The TOF measured on the oscilloscope between the VUV peak and the observed species must be corrected for the transit time from the ionizer to the SEM, through the mass filter. The measured TOF t_{oscillo} can be decomposed into three parts:

1) t_0, from the nozzle to the ionizer chamber of the spectrometer,

2) t_e, from the ionization chamber to the mass filter entrance, where cations are accelerated by the electric field generated by the difference in potential between the ionization chamber wall and the field-axis electrode.

3) t_q, from the quadrupole mass filter to the SEM entrance, where cations have a constant velocity. The multiplication time of electrons

in the SEM, about 10 ns under a 2200-V accelerating potential field, can be neglected with regard to the TOF in the simulation chamber, i.e., about 120 μs.

Combination of the equations of movement for cations in the spectrometer and the kinetic energy theorem in the ionizer source leads to the following equation giving the velocity v_0 of the different species by iteration:

$$\sqrt{\frac{2qV_{\text{Field Axis}}}{m}+v_0^2}+\frac{qV_{\text{Field Axis}}}{md_e}\times\left(-t_{\text{oscillo}}+\frac{d_0}{v_0}+\frac{d_q}{\sqrt{(2qV_{\text{Field Axis}}/m)+v_0^2}}\right)-v_0=0 \quad (1)$$

Differentiating the above equation, we obtain a relative uncertainty $\Delta v_0/v_0$ of 15% from absolute uncertainties $\Delta d_0 = 1$ cm, $\Delta d_e = 1$ mm, $\Delta d_q = 2$ mm, and $\Delta V_{\text{Field Axis}} = 0.1$ V. The absolute uncertainty $\Delta t_{\text{oscillo}}$ is 4 μs, sum of the measurement imprecision (0.5 μs) and the time delay between the effective CO_2 laser firing and the VUV peak produced during the plasma formation in the nozzle (3.5 μs). In comparison, the relative uncertainty on the TOF value optically measured with the two photomultipliers in the chamber is a bit smaller—10%—but the measurement only gives the average velocity of the atomic oxygen present in the beam in the $3p^5$ P excited state. The mass spectrometric TOF method gives the TOF distribution, and at the same time the velocity and energy distributions of all of the atomic oxygen, and more particularly in its ground state.

Fluence Calculation

The fluence of the different species at the spectrometer entrance is calculated from the time distribution recorded on the oscilloscope, after velocity calculation by means of Eq. (1). On the time distribution, the quantity of charges at each point of the timescale under the curve is calculated by the rectangle method and given by

$$N_0(t)=\frac{V(t)\,dt}{eR} \quad (2)$$

The number of cations at the ionization chamber exit is

$$N_c(t)=\frac{N_0(t)}{GT} \quad (3)$$

In other respects, the quantity of cations produced by electron impact in the ionization chamber is[17]

$$N_c(t)=n_e\sigma N_v(t)d \quad (4)$$

So, the particle flux at the spectrometer entrance is given by the following equation:

$$N_s(t)=\frac{V(t)v\,dt}{RGTI\sigma d} \quad (5)$$

The total fluence of particules by pulse at the spectrometer entrance, at 100 cm from the nozzle, is obtained by summing the flux at each point of the timescale. For measurement of the cations already present in the beam before entering the mass spectrometer, the ionizing filament is turned off; consequently, the particules flux is

$$N_s(t)=\frac{V(t)\,dt}{eRGT}\times\frac{4}{\pi d^2} \quad (6)$$

Because the atomic-oxygen source is a point source, the fluence varies in inverse ratio to the squared distances (for both the distance from the nozzle throat, and the radial distance off centerline) as evidenced by erosion of standard materials and quantitative results obtained by LIF on oxygen atoms in the ground state.[8] Accordingly, depending on the experiment geometry that has been used, to evaluate the fluence at 40 cm from the throat nozzle and on the beam centerline, the fluence measured at the spectrometer entrance has been multiplied by a factor of about 1300.

SEM Gain

The SEM gain for different biasing voltages has been obtained from experiment by calculating the ratio of peak intensities recorded with the SEM and the Faraday cup and summed over 100 measurements on the same mass. It has not been possible to measure the SEM gain of fast species in the beam, because the amount of ions collected on the Faraday cup is too small; obtaining a signal measurable on the oscilloscope would have required a high load resistance, thereby raising the time constant of the measuring line in a proportion too large to obtain time resolution of a few tens of microseconds. However, the results concerning the SEM gain and obtained during residual gas analysis can be considered equivalent to those that would have been obtained on the fast beam, as far as the ions analyzed have the same nature and the same kinetic energy at their impact on the conversion dynode of the SEM, which is the case. The ion source parameters indicate that the oxygen atoms enter the mass quadrupole with a kinetic energy of 15 eV. The intensity obtained with the Faraday cup and summed over 100 measurements is 7.74×10^{-11} A. The measured gain varies from 1.5×10^3 to 9.1×10^4, as the polarization voltage is increased from 2 to 3 kV; it is substantially lower than usually measured with this kind of SEM (gain varying from 10^4 to 10^6), probably because of surface degradation of the Cu-Be conversion dynode after a few years of use in a strongly oxidizing environment. For this reason the gain of the SEM had to be checked regularly. Note that this gain calculation takes the efficiency of the deflecting cylindrical condenser into account. The uncertainty related to the SEM gain can be evaluated by the probability of no-creation of secondary electrons by ions on the conversion dynode. This probability can be approached by $e^{-\gamma}$ (Ref. 18), where γ is the number of secondary electrons emitted by the conversion dynode for one incident ion. Taking into account a value of γ between 2 and 4, the probability of no detection of an ion varies respectively from 14 to 2%. Assuming a worst case, the maximum relative uncertainty on G is 20%.

Transmission of the Quadrupole

The transmission of the quadrupole gives the proportion of ions at the exit of the mass quadrupole relative to the number of ions formed in the ionization chamber. Experimentally, this transmission is obtained as the ratio of the ion current intensity measured with the Faraday cup to the theoretical ion current intensity produced in the ionization chamber. The theoretical ion current intensity in the ionization chamber is given by the product $I\,l\,s\,p$ (Ref. 19), which leads in our experimental conditions to a theoretical ion current intensity of about 12×10^{-10} A. The ion current intensity relative to the different species present in the residual gas is measured on the Faraday cup, after selection of a minimum mass resolution allowing transmission of all ion species through the quadrupole mass filter. The measured ionic current intensity is 2.2×10^{-10} A, giving an ion source transmission of 18%, with an uncertainty of 20% attributable to the uncertainty on the pressure and the number of ions produced by centimeter length in the ionization chamber. The quadrupole transmission strongly depends on the entrance experiment conditions of ions, which are the velocity and the angle of incidence. The results concerning the quadrupole transmission obtained during residual gas analysis can be considered equivalent to those that would have been obtained on the fast beam, as far as the ions analyzed have the same 15-eV kinetic energy and angles of incidence are experimentally optimized to be the smallest possible with the propagation axis at their entrance in the quadrupole. Because the fluence is a ratio, the relative uncertainty on it is the sum of the relative uncertainties of the different terms. Relative uncertainties are 20% on the SEM gain, 20% on the ion source transmission, 15% on the velocity, 5% on the voltage measurement, and 10% on the ionization cross section, which leads to a value of about 70% for the relative uncertainty on fluence. Concerning the cations present in the CASOAR beam, the relative uncertainty is lower, about 50%.

These calculated uncertainties are theoretical and do not take into account experimental parameters that are not controllable and reproducible, such as the CO_2 laser energy, the breakdown point of the laser beam into the nozzle, the CO_2 laser firing jitter, and the quantity of oxygen molecules introduced by the fast microvalve.

All of these experimental factors involve an important experimental variability and difficulties in the measurements. For example, contamination problems attributable to the experimental environment inside the chamber, to the chamber opening to the atmosphere, and to the vacuum quality, far from the ultravacuum by the principle of the experiment itself, involve degradation phenomena of the quadrupole rods, which leads to reproducibility problems in its transmission.

Results and Discussion

Experiment Conditions

The beam characterization was performed for the source conditions described in Table 1, delivering a pulsed beam of oxygen atoms, at 2 Hz, and at a velocity of 8 km/s. The atomic-oxygen velocity was adjusted by TOF measurement by mass spectrometry. The optical TOF measured with the two radiometers, under 600-V polarization, was 8.4 μs, giving a 9 km/s velocity for the oxygen atoms in the $3p^5$ P excited state. The electrical signals, visualized on an HP54502A oscilloscope with a 21.5-kΩ load resistance, were averaged over 8 pulses; the oscilloscope was triggered on the CO_2 laser fire command signal; and all TOF measurements were carried out with a SEM polarized at 2600 V.

Neutral Species

During observation of the neutral species, a 300-V potential difference was applied to the deflecting grids situated before the spectrometer entrance, to stop any charged particles from the CASOAR beam having energy less than 1.7 keV. Figures 3–5, obtained after digitization of the TOF distribution obtained on the oscilloscope at a mass-to-charge ratio (m/q) of 32 and numerical treatment, show, respectively, the time distribution of the molecular oxygen fluence

Table 1 Experimental source conditions selected for formation of an atomic-oxygen pulsed beam of 8 km/s velocity

Fire frequency	2 Hz
Time delay between microvalve opening and CO_2 TEA laser firing	455 μs
Molecular oxygen flow	8 cm^3/mn
CO_2 TEA laser energy per pulse	10 ± 5% J
Spot size of the CO_2 TEA laser pulse at the nozzle throat	6 × 4 mm
TOF between the two photomultipliers	8.4 μs

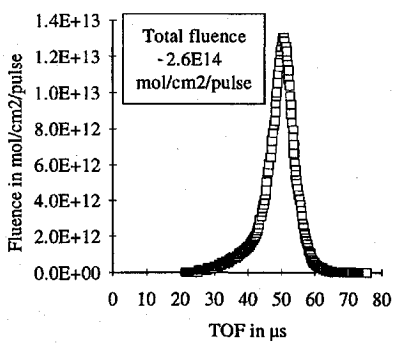

Fig. 3 Time distribution at 40 cm from the nozzle at m/q = 32.

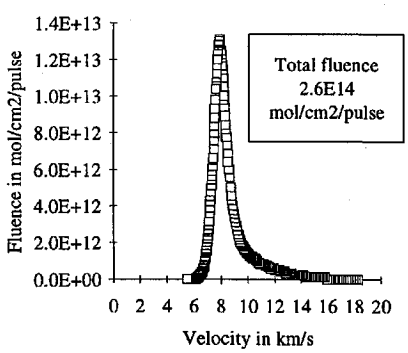

Fig. 4 Velocity distribution at 40 cm from the nozzle at m/q = 32.

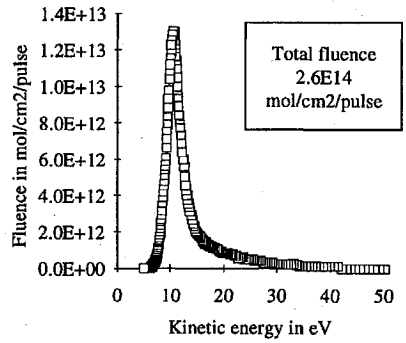

Fig. 5 Kinetic energy distribution of fast O_2 at 40 cm from the nozzle at m/q = 32.

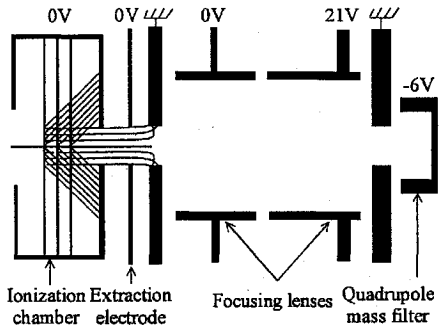

Fig. 6 Trajectory simulation of 0.2-eV thermal molecular oxygen emitted from a cylinder in the spectrometer ion source.

at 40 cm from the nozzle throat, and the velocity and kinetic-energy distributions. The velocity distribution gives an average velocity of 8 ± 1.1 km/s with 1.2 km/s full-width half-maximum (FWHM) value. To consider possible effects attributable to either recombination phenomena of residual atomic oxygen on the walls of the ionization chamber or the presence of residual molecular oxygen, the trajectories of 0.2-eV O_2 molecules in the spectrometer ion source were simulated by the means of SIMION, a software developed by Idaho National Engineering Laboratory, allowing the simulation of ion trajectories in electric and magnetic fields. These simulations, shown in Fig. 6, in which oxygen molecules are emitted from a cylinder in the ionization chamber, enable us to say that thermalized oxygen molecules cannot be observed in the experimental conditions that we have used; thus, they do not disturb the fluence measurement of fast oxygen molecules. Moreover, the high random translational temperature inhibits atomic recombination. The molecular oxygen fluence, calculated at 40 cm from the nozzle throat and on the CO_2 laser axis, gives 2.6×10^{14} molecules/cm^2 per pulse. The amplitude variation in time of the signal averaged out of 8 pulses is less than 5%. The measurement performed with the envelope function on the oscilloscope out of 1000 pulses indicates that the maximum signal amplitude variation is about 20% around the average value; it also shows that the velocity variation is less than 5%. These variations are attributable to fluctuations of the laser energy, varying amounts of molecular oxygen introduced into the nozzle by the fast microvalve per pulse, and a 2- to 3-μs jitter between the laser firing command and the actual laser firing. To further validate the parameter settings of the spectrometer ion source, we simulated the trajectories of 10.6-eV oxygen molecules in the ion source with the employed electrode potentials. This simulation (Fig. 7) shows that the selected potentials in the ion source are quite favorable for a good transmission of 10.6-eV oxygen molecules through the quadrupolar mass filter.

After digitization of the TOF distribution recorded on the oscilloscope at m/q of 16 and numerical treatment, we obtain the time distribution of the atomic-oxygen fluence at 40 cm from the nozzle throat (Fig. 8), as well as the velocity and kinetic energy distributions (Figs. 9 and 10). The velocity distribution shows an average velocity of 8 ± 1.1 km/s with 1.2 km/s FWHM. Because fast oxygen molecules are present in the beam at the same average velocity as the oxygen atoms, dissociation of the molecular oxygen into atomic

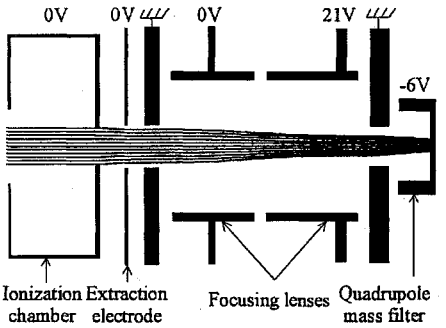

Fig. 7 Trajectory simulation of 10.6-eV fast molecular oxygen in the spectrometer ion source.

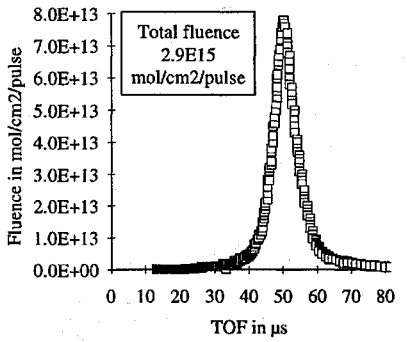

Fig. 8 Time distribution of oxygen-atoms at 40 cm from the nozzle at $m/q = 16$.

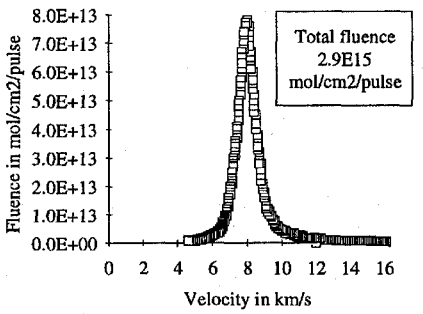

Fig. 9 Velocity distribution of oxygen-atoms at 40 cm from the nozzle at $m/q = 16$.

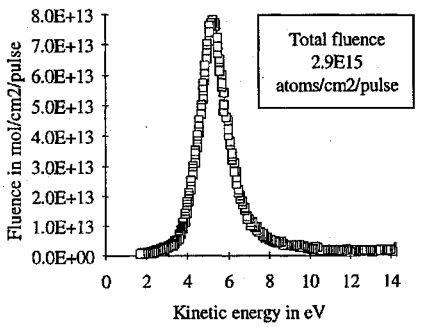

Fig. 10 Kinetic-energy distribution of oxygen-atoms at 40 cm from the nozzle at $m/q = 16$.

oxygen, within the ionization chamber, has to be taken into account to calculate the fluence of the latter. The ratios of the signals obtained at $m/q = 16$ and 32 during the relaxation of the molecular oxygen introduced into the nozzle, with and without the CO_2 laser firing, and not processed in the laser plasma creation, allow us to compute the dissociation rate. The curves in Figs. 11 and 12 show that oxygen molecules not dissociated by the laser pulse have a dissociation percentage of about 5%. These oxygen molecules expanding from 20 bar into a near vacuum should appear 1.3 ms after the VUV spike, corresponding to the isentropic expansion velocity, which is 750 m/s for 300 K room temperature, experimentally measured

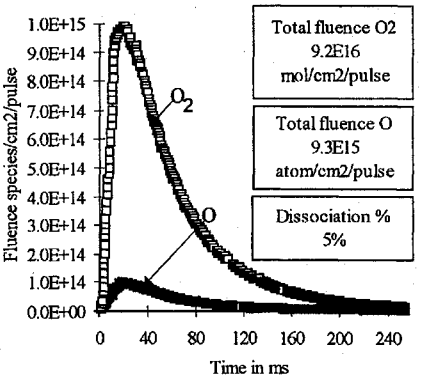

Fig. 11 Time distribution of relaxed oxygen molecules, after laser firing.

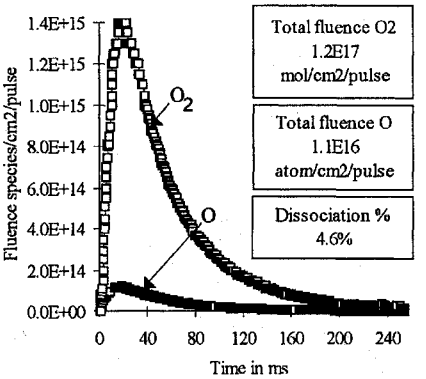

Fig. 12 Time distribution of relaxed oxygen molecules, without laser firing.

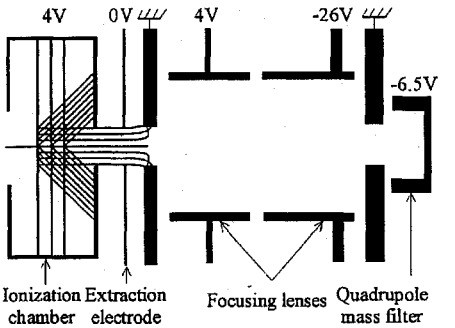

Fig. 13 Trajectory simulation of 0.2-eV thermal oxygen atoms in the spectrometer ion source.

with a piezoelectric pressure transducer 10 cm from the nozzle. The peaks do not appear at 1.3 ms but after 20-ms time delay. This time delay might be the result of the stagnated and thermalized beam flux in the chamber, which would leak into the spectrometer ionization chamber. It might also be attributable to a 2.5-mm-diam diaphragm, located 5 cm in front of the ionization chamber entrance and used to prevent the pressure from rising above 10^{-2} Pa, which makes the flow rate molecular and allows thermalization of the beam flux on the canalization and ionization chamber walls. The dissociation percentage of about 5% is lower than that found in the literature [about 9% (Ref. 19)] because of the difference in the energy of ionizing electrons: 70 eV in our case and 90 eV in the literature. According to this, the atomic-oxygen fluence has been corrected by 5% of the fast O_2 fluence. To consider the residual atomic and molecular oxygen, we simulated the trajectories of oxygen atoms with 0.2-eV energy in the spectrometer ion source, using the SIMION code. The simulation results, shown in Fig. 13, where oxygen atoms are emitted in the ionization chamber by 30-deg steps from a cylinder within 2π spatial angle, enable us to say that residual oxygen atoms cannot be detected and cannot disturb the fluence measurement of fast oxygen-atoms. The oxygen-atom fluence calculation, at 40 cm from the throat of the nozzle and on the CO_2 laser axis, gives 2.9×10^{15}

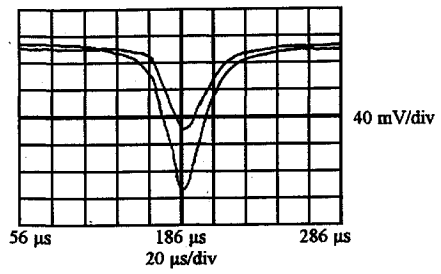

Fig. 14 Fluctuation of the signal obtained for the oxygen atoms out of 1000 pulses.

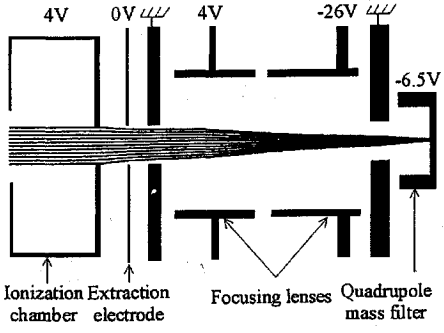

Fig. 15 Trajectory simulation of 5.3 eV fast oxygen atoms in the spectrometer ion source.

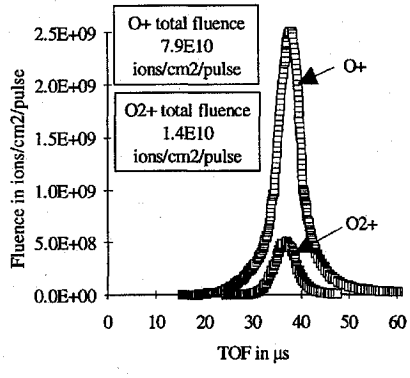

Fig. 16 Time distributions of beam ions at 40 cm from the nozzle at m/q = 16 and 32.

atoms/cm^2 per pulse. The variation of the signal amplitude averaged out of 8 pulses is less than 5%. The measurement realized with the envelope function (Fig. 14) on the oscilloscope, out of 1000 pulses, shows that the total signal amplitude variation is about 25% around the average value. One also can see that the velocity variation is less than 2%. Here also, to validate the parameter settings of the spectrometer ion source found for the best observation of the fast oxygen atoms, we simulated the trajectories of 5.3-eV oxygen-atoms in the ion source with the exact potentials employed for measurement. Simulation results (Fig. 15) show that these settings of the ion source enable us to have favorable conditions for transmission of 5.3-eV oxygen atoms through the quadrupole mass filter.

Ionic Species

For the observation of the ionic species present in the beam of CASOAR, no potential difference was applied to the deflecting electrodes, and the ionizing electron emission was turned off. Figure 16 shows the time distribution at 40 cm from the nozzle throat at m/q of 16 and 32, as well as the velocity and kinetic-energy distributions (Figs. 17 and 18). The velocity distribution gives an average velocity of 10.6 ± 1.5 km/s with 1.4 km/s FWHM for the O^+ ions, and an average velocity of 10.9 ± 1.5 km/s with 1.6 km/s FWHM for the O_2^+ ions. Here, the fluence calculations are not affected by problems of recombination or dissociation, because of the absence of ionizing electrons in the mass-spectrometer ion source. The fluence, at 40 cm from the throat of the nozzle and on the CO_2 laser axis, is 7.9×10^{10}

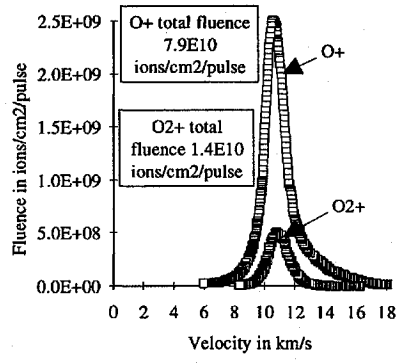

Fig. 17 Velocity distribution of beam ions at 40 cm from the nozzle at m/q = 16 and 32.

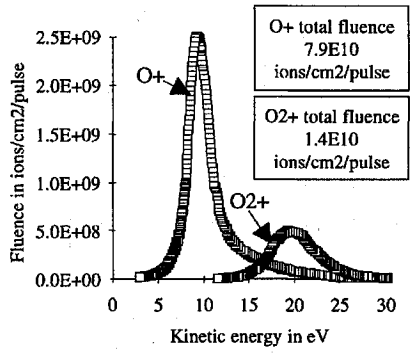

Fig. 18 Kinetic-energy distribution of beam ions at 40 cm from the nozzle at m/q = 16 and 32.

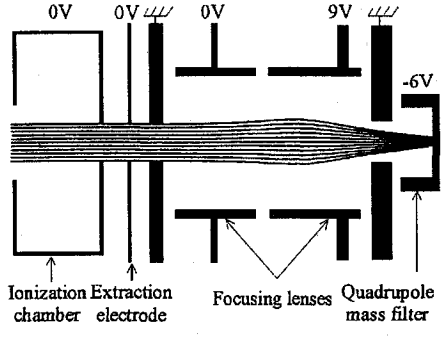

Fig. 19 Trajectory simulation of O^+ cations of 9.3-eV translational energy in the spectrometer ion source.

ions/cm^2 per pulse for O^+ and 1.4×10^{10} ions/cm^2 per pulse for O_2^+. The variation of the signal amplitude averaged out of 8 pulses is less than 5%. The measurement realized with the envelope function on the oscilloscope, out of 1000 pulses, shows that the signal amplitude variation is about 20% around the average value. It also indicates that the velocity variation is less than 5%. The ion trajectories with 9.3-eV energy for O^+ (Fig. 19) and with 19.8-eV energy for O_2^+ in the ion source again show good conditions for ions transmission through the quadrupole.

Summary of Findings

In optimized working conditions, selected to deliver a pulsed beam of oxygen atoms at 8 km/s in the CASOAR simulator, material sample subjected to testing and placed at 40 cm from the nozzle throat, at 1 cm from the centerline, is exposed to a pulsed beam that is composed of several elements successively received in the course of time. First, it receives VUV photons, created in the initial plasma formation process, whose wavelength is in the range of 60–120 nm with a total fluence estimated to be half the one of oxygen atoms, i.e., 1.4×10^{15} photons/cm^2 per pulse.[16] This important fluence of far-uv photons, whose action in synergy with fast oxygen atoms has been shown,[16,20,21] can constitute a concern when testing some special materials. Second, 37 μs later, the sample receives O^+ and

Table 2 Different species in the atomic-oxygen pulsed beam at 8 km/s velocity

Species	Velocity, km/s	Fluence per pulse, species/cm^2	Relative quantity
O	$8 \pm 15\%$	2.9E15	91%
O_2	$8 \pm 15\%$	2.6E14	9%
O^+	$10.6 \pm 15\%$	7.9E10	25 ppm
O_2^+	$10.9 \pm 15\%$	1.4E10	5 ppm

O_2^+ ions having the same average velocity, about 10.9 ± 1.5 km/s, with fluences about 10^{11} ions/cm^2 per pulse. Then, 10 μs after the ions, the sample is exposed to fast oxygen atoms and molecules with the same average velocity, about 8 ± 1.1 km/s, with respective fluences 2.9×10^{15} atoms/cm^2 and 2.6×10^{14} molecules/cm^2 per pulse. Finally, the sample receives, after a 0.5-ms delay time, the rest of the molecular oxygen, not dissociated by the laser energy, about 2.9×10^{16} molecules/cm^2 per pulse, with an average velocity of 750 m/s. These results completely agree with those realized by Minton et al.[11] on the same Physical Sciences, Inc., atomic-oxygen source by mass spectrometry, which showed the VUV photons, the TOF distributions of the fast oxygen atoms and molecules. From the ratio of fluences obtained for relaxed molecular oxygen, with and without laser firing (Figs. 11 and 12), one can estimate that 24% of the oxygen molecules introduced into the nozzle are involved in the plasma formation process. Fluences and velocity of the different species are summarized in Table 2; they are in good agreement with earlier rough estimates made by Caledonia et al.[7] The TOF measurement allowed to know the velocity of the different species with a relative uncertainty of 15%. This uncertainty is in the same order of magnitude as that obtained by TOF optical measurement, with photomultipliers detecting excited oxygen atoms in the O $3p^5$P state. However, the velocity of 9 km/s obtained by TOF optical measurement is different from the 8-km/s velocity obtained by mass spectrometry measurement, in the same experimental conditions. Ionic species about 11 km/s are present in the beam; likewise, there are probably excited oxygen atoms incoming from electronic recombination of part of the slower ions and then having a greater velocity than that of atomic oxygen in the ground state. Because TOF distribution analysis by mass spectrometry does not allow us to differentiate oxygen atoms in their different excitation states, the velocity distribution of the excited atomic oxygen with 9 km/s average velocity is included in the velocity distribution obtained by mass spectrometry with 8 km/s average velocity and 1.2 km/s FWHM.

Conclusion

The characterization of an energetic oxygen-atom pulsed beam by quadrupolar mass spectrometry allowed us to demonstrate some potentialities of this technique, which are the qualitative analysis, TOF measurements, and quantitative measurements. The qualitative analysis of the atomic-oxygen pulsed beam at 8 km/s displayed the different species (ions and neutrals) with a mass resolution lower than unity, as well as the presence of far-uv photons. The mass spectrometry TOF measurements gave a good accuracy on the velocity distribution of oxygen atoms present in the beam. The fluence and velocity measurements confirmed that the simulation chamber is well adapted to the study of the action of the oxygen atom on spacecraft materials, enabling us to simulate the action of LEO 5-eV oxygen atoms with acceptable acceleration factors. The presence of fast cations that could disturb the study of the action of fast ground atomic oxygen on materials, although being in minor quantity, can be suppressed easily, for instance, by placing some polarized deflecting plates in front of the samples. The presence of far-uv photons, whose action in synergy with fast atomic oxygen on fluorinated polymers has been shown, can constitute a concern when testing some special materials. Further studies in this respect should be carried out, for example, studies related to possible effects of fast O_2 molecules on materials in presence of the far-VUV photons emitted by the source. Furthermore, the quadrupolar mass spectrometry appears promising concerning the analysis of oxidation products emitted by materials exposed to a pulsed beam of energetic oxygen atoms similar to the one used in this study but in a different configuration.

References

[1]Koontz, S. L., Albyn, K., and Leger, L. J., "Atomic Oxygen Testing with Thermal Atom Systems: A Critical Evaluation," *Journal of Spacecraft and Rockets*, Vol. 28, No. 3, 1991, pp. 315–323.

[2]Koontz, S. L., Albyn, K., and Leger, L. J., "Materials Selection for Long Life in Low Earth Orbit," *Journal of the Institute of Environmental Sciences*, Vol. 33, March–April 1990, pp. 50–59.

[3]Cross, J. B., and Blais, N. C., "High Energy/Intensity CW Atomic Oxygen Beam Source," *Rarefied Gas Dynamic: Space-Related Studies*, edited by E. P. Mundt, D. P. Weaver, and D. H. Campbell, Vol. 116, Progress in Aeronautics and Astronautics, AIAA, Washington, DC, 1989, pp. 143–155.

[4]Cross, J. B., Koontz, S. L., Gregory, J. C., and Edgell, M. J., "Hyperthermal Atomic Oxygen Reactions with Kapton and Polyethylene," *Materials Degradation in Low Earth Orbit (LEO)*, edited by B. A. Banks and V. Srinivasan, Minerals, Metals, and Materials Society, Warrendale, PA, 1990, pp. 1–13.

[5]Orient, O. J., Chutjian, A., and Murad, E., "Recombination Reactions of 5-eV O(^{3}P) Atoms on a MgF_2 Surface," *Physical Review A: General Physics*, Vol. 41, April 1990, pp. 4106–4108.

[6]Banks, B. A., Rutledge, S. K., and Brady, J. A., "The NASA Atomic Oxygen Effects Test Program," *Proceedings of the 15th Space Simulation Conference*, NASA CP-3015, Williamsburg, VA, 1989, pp. 51–65.

[7]Caledonia, G. E., Krech, R. H., and Green, B. D., "A High Flux Source of Energetic Oxygen Atoms for Material Degradation Studies," *AIAA Journal*, Vol. 25, No. 59, 1987, pp. 59–63.

[8]Peze, P., "Characterization of an Atomic Oxygen Pulsed Beam by Laser Induced Fluorescence," Thesis, No. 118, Ecole Nationale Supérieure de l'Aéronautique et de l'Espace, Toulouse, France, Sept. 1993, pp. 1–135.

[9]Hunton, D. E., Trzeinski, E., Cross, J. B., Spangler, L. H., Hoffbauer, M. A., Archuleta, F. H., and Visentine, J. T., "Mass Spectrometers and Atomic Oxygen," *Proceedings of the NASA Workshop on Atomic Oxygen Effects*, edited by D. E. Brinza, Jet Propulsion Lab., Publication 84-14, California Inst. of Technology, Pasadena, CA, 1987, pp. 21–28.

[10]Sonoda, K., Nishikawa, T., and Nakanishi, K., "Atomic Oxygen Effect on Physical Properties of Spacecraft Materials in Low Earth Orbit," *AIAA 24th Thermophysics Conference* (NewYork), AIAA, Washington, DC, 1989 (AIAA Paper 89-1761).

[11]Minton, T. K., Nelson, C. M., Brinza, D. E., and Liang, R. H., "Inelastic and Reactive Scattering of Hyperthermal Atomic Oxygen from Amorphous Carbon," Jet Propulsion Lab., NASA Publication 91-34, California Inst. of Technology, Pasadena, CA, Aug. 1991, pp. 1–30.

[12]Cross, J. B., Koontz, S. L., and Hunton, D. E., "Flight Mass-Spectrometer Calibration in a High-Velocity Atomic-Oxygen Beam," *Journal of Spacecraft and Rockets*, Vol. 32, No. 3, 1995, pp. 496–501.

[13]Hunton, D. E., and Calo, J. M., "Low Energy Ions in the Shuttle Environment: Evidence for Strong Ambient-Contaminant Interactions," *Planetary and Space Science*, Vol. 33, No. 8, 1985, pp. 945–951.

[14]Strganac, T. W., Letton, A., Rock, N. I., Williams, K. D., and Farrow, D. A., "Characterization of Polymer Films Retrieved from NASA's Long Duration Exposure Facility," *Journal of Spacecraft and Rockets*, Vol. 32, No. 3, 1995, pp. 502–506.

[15]Koontz, S. L., Leger, L. J., Visentine, J. T., Hunton, D. E., Cross, J. B., and Hakes, C. L., "EOIM-III Mass Spectrometry and Polymer Chemistry: STS 46, July–August 1992," *Journal of Spacecraft and Rockets*, Vol. 32, No. 3, 1995, pp. 483–495.

[16]Weihs, B., and Van Eesbeek, M., "Secondary VUV Erosion Effects on Polymers in the ATOX Atomic Oxygen Exposure Facility," *Proceedings of the sixth International Symposium on Materials in a Space Environment*, European Space Research and Technology Centre, European Space Agency, Noordwijk, The Netherlands, 1994, pp. 277–283.

[17]Goeringer, D. E., Glish, G. L., and McLuckey, S. A., "Fixed-Wavelength Laser Ionization/Tandem Mass Spectrometry for Mixture Analysis in the Quadrupole Ion Trap," *Analytical Chemistry*, Vol. 63, No. 13, 1991, pp. 1186–1192.

[18]Thirkell, L., "Analyse Quantitative d'Echantillons Geologiques par une Technique SIMS Quadripolaire: Etude de l'Effet de Matrice," Thesis, Université d'Orléans, France, Sept. 1991, pp. 1–159.

[19]Balzers, S. A., "Mesures de Pressions Partielles dans la Technique du Vide," Balzers S. A., No. BG 800 169 PF, Meudon, France, 1990, pp. 1–32.

[20]Koontz, S. L., Leger, L. J., Albyn, K., and Cross, J. B., "Vacuum Ultraviolet Radiation/Atomic Oxygen Synergism in Materials Reactivity," *Journal of Spacecraft and Rockets*, Vol. 27, No. 3, 1990, pp. 346–348.

[21]Cross, J. B., and Koontz, S. L., "Ground-Based Simulation of LEO Environment: Investigation of a Select LDEF Material-FEP Teflon^{TM}," *Proceedings of a NASA Conference on LDEF Materials Results for Spacecraft Applications*, NASA CP-3257, Huntsville, AL, 1992, pp. 379–389.

I. D. Boyd
Associate Editor